DETAILED NEUTRONIC MODELLING OF THE CROCUS RESEARCH REACTOR USING APOLLO3® TRANSPORT CODE

Igor Zmijarevic[1], **Mereke Tontayeva**[2*], **Daniele Tomatis**[1] **and Zarko Stankovski**[1]
[1]DEN-Service d'études des réacteurs et de mathématiques appliquées (SERMA)
CEA-Saclay, Université Paris-Saclay, F-91191 Gif-sur-Yvette, France
[2]IMT ATLANTIQUE, Bretagne - Pays de la Loire, École Mines-Télécom,
La Chantrerie, 4 rue Alfred Kastler, BP 20722, 44307 Nantes Cedex 3, France

igor.zmijarevic@cea.fr, mtontayeva@gmail.com, daniele.tomatis@cea.fr, zarko.stankovski@cea.fr

ABSTRACT

The deterministic transport code APOLLO3® developed at CEA was used to setup the 2D and 3D neutronic models of the zero-power, water-moderated experimental reactor CROCUS, operated by Swiss Federal Institute of Technology in Lausanne, in order to verify the computational methodology and apply it to the interpretation of experiments conducted under the CORTEX European project related to neutron noise measurements in which CEA participates. The variants of the self-shielding calculation based on fine structure method were analysed and a fully heterogeneous 2D description of the reactor is tested with different discretisation options using the method of characteristics. The homogeneous model intended for the discrete ordinates, short characteristic calculation is also analysed with the emphasis on the production of equivalent cross sections. The reaction rates preserving equivalent cross sections are set on the basis of the whole 2D domain used as reference homogenisation problem.

KEYWORDS: APOLLO3® transport code, CROCUS reactor, MOC, short characteristics, homogenisation

1. INTRODUCTION

The CROCUS experimental reactor, powered by the Swiss Federal Institute of Technology, Lausanne, is a light water moderated critical assembly with a two-zone core containing oxide and metallic uranium fuel pins. This is a reactor of a small size, approximately of cylindrical shape in which the criticality conditions are reached by changing the water level. The reactor has been used for many experiments and some of these have been approved as benchmark configurations and published in the international community, thus allowing the verification of computer codes and nuclear data [1]. Besides a constant effort by the APOLLO3® development group to enrich the validation base of the code with a variety of reactor configurations, a particular interest in CROCUS reactor is in the ongoing experimental program of the reactor noise measurement, which is a part of the European project CORTEX in which CEA participates.

*Present address: tontayeva@nnc.kz

Two different approaches of the reactor noise calculations have been implemented in APOLLO3®, one in the frequency domain using the transport and diffusion flux solutions in 2D and 3D homogenised geometries[2], and another in temporal domain with the flux solutions in 2D heterogeneous configurations[3]. The interpretation of the experiment will comprise the calculation of CROCUS using these two options.

The work presented here is out of the scope of reactor noise analysis and focuses on the calculation methodology of this particular reactor in a general case that will be later adapted to a given experiment. This is considered as a preliminary step having objective to analyse different possibilities to model the CROCUS reactor and to setup a comprehensive calculation scheme that gives the precise answers about the reactivity, the reaction rates and flux distributions that will allow an easy comparison with reactor measurements to be performed in foreseen campaigns.

Among many possibilities that offers the APOLLO3® as a modular code, the attention is oriented toward the self-shielding calculation options, the choice of the fully heterogeneous two-dimensional reactor model, the homogenisation procedure and the three-dimensional homogenised model. Two flux solvers that have noise calculation capability are the 2D variant of the TDT, a method of characteristic (MOC) module [4] and the 2D/3D variant of the IDT, discrete ordinates code that uses homogeneous Cartesian meshes. [5]

Recent CROCUS calculations[6,7] that are based on the classical approach of cross section homogenisation with the three-dimensional calculations using the two-group diffusion theory may not provide satisfactory results for the detailed reaction rate distributions. The renewed scheme relies on accurate Monte Carlo calculations for the production of homogenised cross sections but still using diffusion theory. Such obtained results still show the discrepancies of around 400 pcm in reactivity and more than 10 % in pin-wise power distribution. Increase in number of groups (up to 40), but still relying on diffusion approximation, does not provide a significant improvement.

Our classical approach is extended to the whole-reactor 2D heterogeneous transport calculations for the production of homogenised cross sections, which is expected to reduce these errors by an order of magnitude. The 2D results presented here show the discrepancies of about 100 pcm in reactivity and around 1% in pin-wise fission rates compared to TRIPOLI-4® Monte Carlo results.[8]

2. TWO-DIMENSIONAL REACTOR MODEL

Contrarily to the power producing LWRs, the particular design of the CROCUS reactor with a non-uniform lattice and a relatively small core makes the standard two-step calculation procedure difficult to apply. On the other hand, the increased moderation due to higher water-to-fuel volume ratio, the low operating temperature and higher fuel density (metallic fuel of the outer core) require a careful spatial discretization for the flux calculation.

2.1. Self-shielding

Among different possibilities to perform the self-shielding calculations that have been implemented in APOLLO3®, namely the sub-group method, Tone's method, and the classical fine-structure method, all based on extensive use of probability tables, we opted for the latter in this

work. The reason is that the isotopic composition is relatively simple, only ^{238}U and ^{235}U as heavy isotopes and a low enrichment that makes the effect of resonance interferences weak. Also, the first two methods are efficient when the group width is small, which would involve at least a 383-group APOLLO3® library. In the CROCUS case we also intend to perform the calculations without the group collapsing so we use the 281-group SHEM multigroup data library [9] for which the chosen self-shielding method is suitable. Nevertheless, the absence of light nuclei in the metallic fuel may compromise the basic assumption of the fine structure approach, which models a dilution of a resonant isotope in the moderator. In this case, while calculating the effective cross sections of one isotope, the other plays the role of moderator. This method, referred as of Livolant-Jeanpierre, [10] consists in solving the fine structure equation derived from the slowing down equation describing the homogeneous mixtures of a resonant isotope and moderator. The spatially heterogeneous problem is solved using the collision probability method without the need of a Dancoff correction. The approximations that make the solution efficient in practice are related to the slowing down model and the numerical quadrature used for reaction rate calculation. In order to correct this approximation, an equivalence procedure is used where an equivalent reaction rate preserving background cross section of a homogeneous medium is found using the same slowing down model and the quadrature formulas. This background cross section is then used to obtain the reaction rate from the temperature dependent interpolation tables. These tabulated values are calculated by the GALILEE processing tool [11], based on the NJOY Nuclear Data Processing System. These are calculated using very fine energy mesh and are considered accurate.

The preliminary tests have been conducted separately for the two kinds of fuel in infinite lattice configurations in order to assess the validity of the self-shielding options. The spatial dependence of the effective cross sections have been analysed and optimised by varying the number of concentric annuli in the fuel having different self-shielded cross section. The radii are chosen such that in the case of 20 fuel rings, considered as reference mesh, the volume of each ring is 5% of the fuel volume. The coarser mesh is then chosen by de-refining the reference one. The four-annulus case, for example, has the volume fractions of 50, 30, 15 and 5 percent of the fuel volume going from the centre outward. The number of regions for flux calculation is optimized by varying the number of regions in water, using equidistant radial points, and the number of sectors. The examples of these meshes is shown in Fig. 1.

The variation of the multiplication factor with the mesh refinement is shown in Table 1 for different number of rings (self-shielding regions) in fuel and number of sectors. The results for oxide fuel cells show good agreement with Monte Carlo reference, which is 4 pcm difference in reactivity, while for metallic fuel this method gives a discrepancy of around 130 pcm.

Figs. 2 and 3 illustrate the accuracy of absorption rates obtained in single cell calculations. The case corresponds to a very fine spatial mesh comprising 20 annular regions in fuel and 18 in water. The flux is calculated using the MOC solver with P_3 anisotropic scattering. The plotted difference in absorption rates per isotope between APOLLO3® (A3) and TRIPOLI-4®(T4) results, $\tau^g_{a,\text{A3}} - \tau^g_{a,\text{T4}}$, where $\tau^g_a = \langle \Sigma^g_a, \phi^g \rangle_{\text{fuel}}$ is the volume integrated absorption rate of each resonant isotope. The flux is normalized to a unit production, such that the difference in integrated absorption rate directly gives the contribution to the reactivity difference between two calculations, i.e. $\Delta(1/k_{\text{eff}})$. The 281-group SHEM energy mesh allows to refrain from self-shielding calculation at the energies below 22.5 eV (above energy group number 93). It can be seen that the group wise error generated

on ^{235}U and ^{238}U in the oxide fuel is merely 10 pcm. A few pcm is visible in the vicinity of the great 6.67 eV resonance of ^{238}U (group 167), where self-shielding calculation is absent. This error is even smaller than those observed in much lower energies where the dominant process is thermalisation. On the contrary, the metallic fuel shows a 40 pcm difference in the group 80 ($\approx$ 162-198 eV). In-here and in the neighbouring groups there are multiple resonances within each group, which together with the absence of a moderating isotope and increased concentration of uranium isotopes in the metal produces the errors larger than in UO_2.

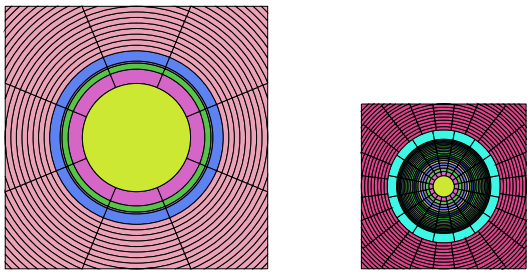

Figure 1: Example of spatial mesh used for cell analysis. The colours in fuel designate different self-shielding regions.

Table 1: Errors in effective multiplication factor $\Delta k = k_{\text{eff,A3}} - k_{\text{eff,T4}}$ ($\sigma_{\text{T4}} \approx$ 5 pcm)

Number of rings/sectors	Δk (pcm)	
	metal fuel	oxide fuel
4 / 4	364	87
4 / 8	271	43
6 / 8	241	46
6 / 12	237	47
10 / 12	174	11
10 / 16	173	11
20 / 16	151	6
20 / 24	137	4

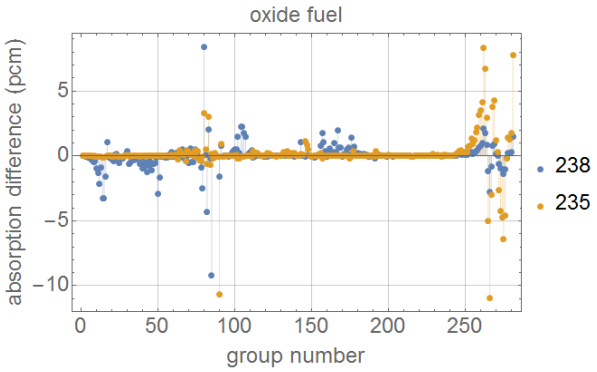

Figure 2: ^{238}U and ^{235}U absorption rate differences in oxide fuel (in pcm).

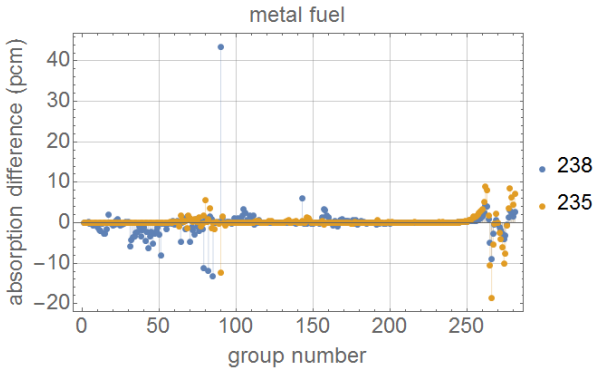

Figure 3: ^{238}U and ^{235}U absorption rate differences in metal fuel (in pcm).

The spatially dependent self-shielding effects in the real geometry would require the full collision probability formulation in order to account for the interaction of the pins of different kinds at different positions, which remains computationally rather expensive. Therefore, this is done approximatively using a simplified geometry model shown in Fig. 4 that comprises a 2D array of UO_2 and metallic fuel pin cells, water gap and reflector. This is a "quasi one-dimensional model", where the four layers of UO_2 and the two and a half layers of U-metal cells are put together in order to preserve the relative volume ratio in radial direction such to represent an array of pins from the centre of the core outwards. The motif is calculated using the reflective boundary condition. Four self-shielding regions in each pin are chosen and differentiated per pin. Thus, eleven different UO_2

and three U-metal pin are assigned a total of 56 different cross sections sets. The colours in Fig. 4 in fuel designate these 56 different self-shielding regions. These are then dispatched in the actual core layout trying to respect the relative position of fuel within the core as shown in Fig. 5

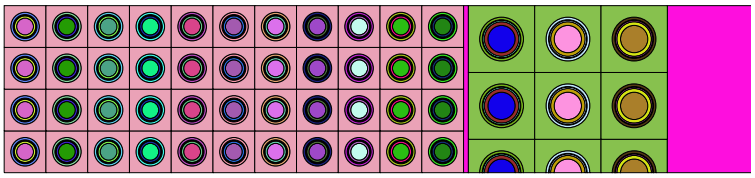

Figure 4: Simplified geometry model for self-shielding calculation. The colours of fuel zones indicate different self-shielding regions. The reflector zone is truncated in this image.

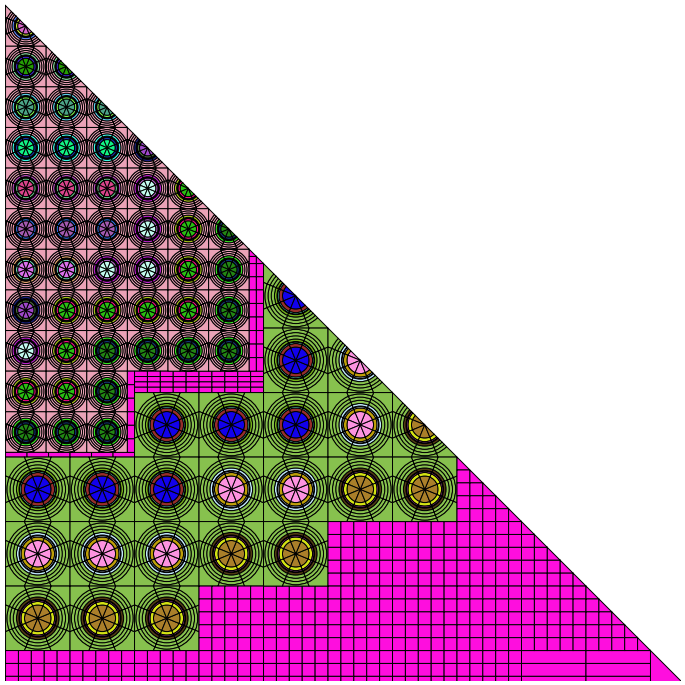

Figure 5: Example of the MOC spatial mesh in a 2D heterogeneous geometry model. The colours in fuel pins indicate different self-shielding regions adopted for this calculation. The image is truncated over the reflector zone.

2.2. 2D Core Calculations

Fig. 5 shows the example of the MOC spatial mesh on the eightfold symmetric geometric domain. The results of one of parametric studies involving different MOC integration parameters and different orders of scattering anisotropy are summarized in Table 2. The TRIPOLI-4® reference calculation was run with the pin wise fission rate distribution in output.

The discrepancy of the asymptotic solution is in the agreement with the error observed on the

single cells calculations in which the principal source of error is the self-shielding model. One may conclude that the MOC approximation does not introduce any further bias. The pin-wise reaction rate errors are shown in Figs. 6 and 7. Maximum relative error is around 1% with the RMS of relative errors equal 0.5%. The errors are presented separately for oxide and metal fuel in Tables 3 and 4 and RMS in Table 5.

Table 2: Errors in effective multiplication factor compared to Monte Carlo reference (in pcm) for various scattering anisotropy orders (P_n) and different MOC quadratures. (N_φ and Δr are respectively number of azimuthal angles and trajectory spacing.)

P_n	MOC quadrature ($N_\varphi, \Delta r$ [mm])								
order	16, 0.5	16, 0.25	16, 0.1	20, 0.5	20, 0.25	20, 0.1	24, 0.5	24, 0.25	24, 0.1
0	-1120	-1173	-1171	-1110	-1166	-1180	1075	-1113	-1121
1	-225	-287	-286	-223	-283	-300	-205	-257	-262
3	-94	-157	-156	-90	-152	-168	-74	-127	-132
5	-90	-152	-151	-85	-146	-163	-68	-121	-126

Table 3: Maximum pin-wise fission rate relative error (in %) for various scattering anisotropy orders and different MOC quadratures in oxide fuel pins.

P_n	MOC quadrature ($N_\varphi, \Delta r$ [mm])								
order	16, 0.5	16, 0.25	16, 0.1	20, 0.5	20, 0.25	20, 0.1	24, 0.5	24, 0.25	24, 0.1
0	-0.67	-0.70	-0.70	-0.71	-0.68	-0.70	-0.70	-0.72	-0.72
1	-0.58	-0.61	-0.62	-0.62	-0.60	-0.61	-0.60	-0.62	-0.62
3	-0.62	-0.65	-0.65	-0.66	-0.63	-0.65	-0.64	-0.66	-0.66
5	-0.62	-0.65	-0.65	-0.66	-0.64	-0.65	-0.64	-0.66	-0.66

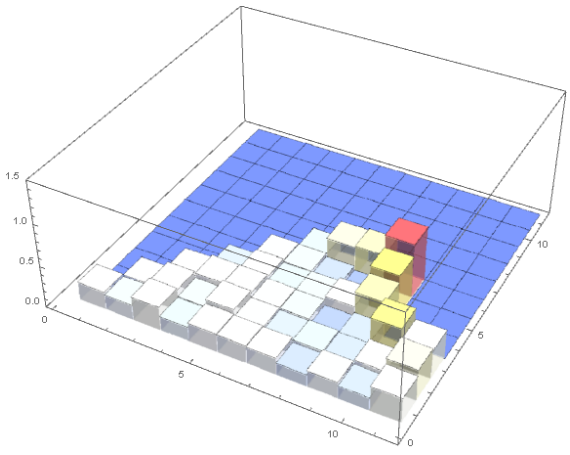

Figure 6: Fission rate relative errors in oxide fuel (in%).

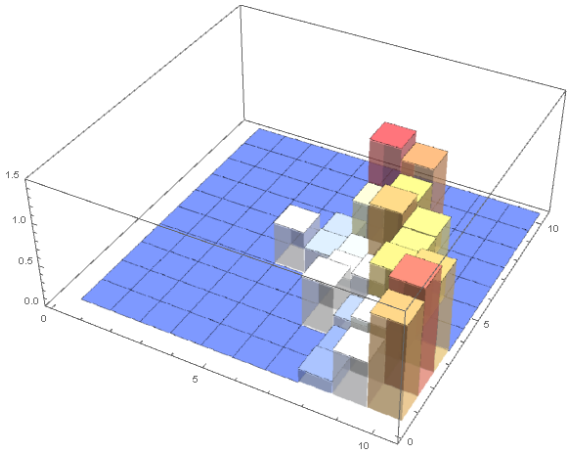

Figure 7: Fission rate relative errors in metal fuel (in%).

Table 4: Maximum pin-wise fission rate relative error (in %) for various scattering anisotropy orders and different MOC quadratures in metallic fuel pins.

P_n	MOC quadrature ($N_\varphi, \Delta r$ [mm])								
order	16, 0.5	16, 0.25	16, 0.1	20, 0.5	20, 0.25	20, 0.1	24, 0.5	24, 0.25	24, 0.1
0	1.79	1.73	1.75	1.78	1.74	1.72	1.69	1.63	1.69
1	1.63	1.70	1.73	1.64	1.66	1.72	1.57	1.64	1.70
3	1.30	1.32	1.36	1.30	1.30	1.35	1.25	1.25	1.31
5	1.31	1.33	1.37	1.32	1.32	1.36	1.26	1.27	1.32

Table 5: RMS of relative errors in fission rates per pin compared to TRIPOLI-4® reference (in %) for various scattering anisotropy orders and different MOC quadratures.

P_n	MOC quadrature ($N_\varphi, \Delta r$ [mm])								
order	16, 0.5	16, 0.25	16, 0.1	20, 0.5	20, 0.25	20, 0.1	24, 0.5	24, 0.25	24, 0.1
0	0.64	0.62	0.63	0.66	0.63	0.63	0.62	0.60	0.63
1	0.67	0.68	0.69	0.66	0.66	0.68	0.64	0.65	0.68
3	0.50	0.52	0.54	0.50	0.50	0.53	0.48	0.50	0.52
5	0.51	0.52	0.54	0.51	0.50	0.53	0.49	0.50	0.53

3. HOMOGENEOUS MODEL

In order to construct a 3D homogeneous model, a pin-wise homogenisation is done using the above shown 2D heterogeneous solution. Each fuel cell is homogenised separately using its local flux such that there is 68 different cross sections sets for fuel regions in the eight-fold symmetric motif of the reactor, another five zones representing the water gap between the inner and outer core and another five zones representing the reflector. Different multigroup structures have been investigated with the number of energy groups varying between 26 and 281. The homogeneous flux calculation uses short characteristics method with the linear flux expansion, S_8 Chebyshev-Legendre quadrature with P_3 scattering anisotropy. Simple flux and volume weighting produces the errors in reactivity between 300 and 400 pcm with the pin-wise rate distribution errors that reach 3 %. Table 6 shows the reactivity errors for different spatial discretization in different multigroup structures. The results that are all within 75 pcm interval, suggest that the flux solver options are quite adequate, but the quality of cross sections produced by flux and volume weighting is compromised. Figs. 8 and 9 illustrate the errors in pin-wise production rate distribution for the case of 1 cm max. mesh size, compared to direct heterogeneous 281-group reference. Most of these discrepancies are situated in the fuel around the internal water gap and at the core-reflector interface, where the increased thermalisation induce very strong flux gradients. Indeed, this can be observed in the flux distribution shown in Fig. 10. This is the result of 281-group calculation with the plot shown for the group 269 of the SHEM mesh, which is the energy interval (0.0554982, 0.0651994) eV, where the maximum of the thermal flux in water regions occurs, both in internal gaps and reflector.

Table 6: Reactivity errors (in pcm) of homogeneous calculation using flux and volume weighting calculated by linear short characteristics with P_3 scattering.

max. mesh size (cm)	number of collapsed groups		
	26	44	281
2	390	374	320
1	390	374	327
0.5	380	366	316
0.25	376	372	316

The remedy to this problem is the application of the equivalence procedure [12], where the equivalence coefficients are sought iteratively using the fixed point iterations. Again, the whole computational domain is used as reference homogenisation problem searching thus an equivalence coefficient per homogenised zone and energy group. The errors in reaction rates using equivalent cross sections are reduced to the order of 10^{-5}. Fig. 11 shows the equivalence factors for different oxide and metallic fuel pin cells situated along the axis of the reactor. Significant elongation from the value of 1.0 happens in the deep thermal energy range in the whole core and the dips can be observed around the position of the lowest ^{238}U resonances. We consider such modified equivalent cross sections acceptable.

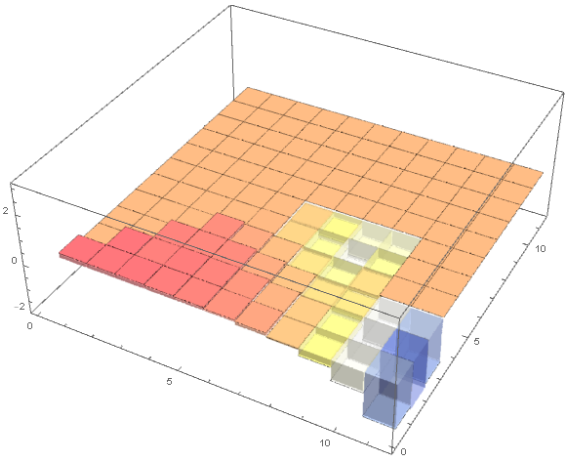

Figure 8: Pin-wise production rate ($\nu\Sigma_f\phi$) relative errors in oxide fuel (in %) using homogenisation without equivalence.

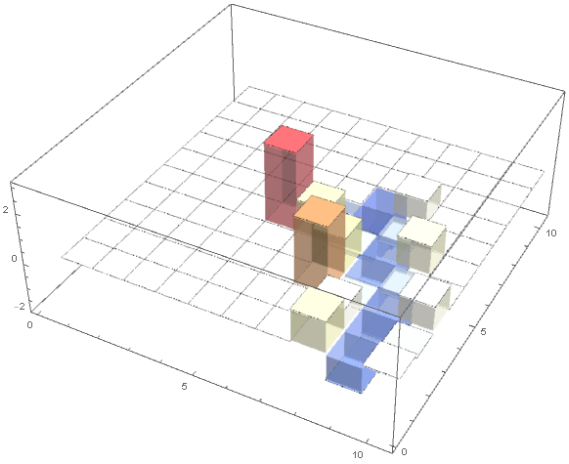

Figure 9: Pin-wise production rate ($\nu\Sigma_f\phi$) relative errors in metal fuel (in %) using homogenisation without equivalence.

4. CONCLUSIONS

This work represents the preliminary activities in order to set an efficient calculation scheme for the CROCUS reactor that will be used for the interpretation of measurements. Heterogeneous

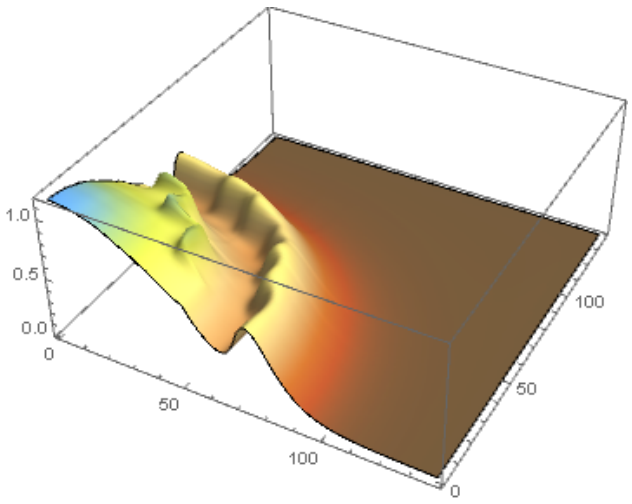

Figure 10: Thermal flux distribution in a quadrant of a 2D reactor model at the energy of flux maximum in the water gaps and reflectors. (Flux is in arbitrary units, mesh numbers on abscissae.)

2D model gives satisfactory results, although further improvements are possible, especially in the self-shielding applied to the metallic fuel, e.g. the subgroup method instead of the fine structure one. Current results for this fuel gives the reactivity discrepancy of about 100 pcm, while for the oxide fuel the model proved to be suitable. A fully heterogeneous reactor representation calculated by the method of characteristics shows good agreement in fission rate distribution with the Monte Carlo reference. The corresponding model is also set for the homogeneous transport calculations, where a strong homogenisation effect is observed that alters the reaction rates distribution at the fuel regions around the strong flux gradients. We showed that the equivalence procedure is able to produce the correction factors not far from unity even in the case of 281-group homogenisation. This means that this calculation scheme is suitable for three dimensional homogenised model that is currently in progress.

ACKNOWLEDGEMENTS

This work forms part of the CORTEX project which has received funding from the Euratom Research and Training Programme 2014-2018 under grant agreement No 754316.

REFERENCES

[1] U. Kasemeyer, et al., "Physics of Plutonium Recycling, Volume IX, Benchmark on Kinetic Parameters in the CROCUS Reactor," OECD/NEA Nuclear Science Committee, NEA No. 4440, OECD 2007, ISBN 978-92-64-99020-3, https://www.oecd-nea.org/science/pubs/2007/nea4440-CROCUS.pdf

[2] A. Rouchon et al., "The new 3-D multigroup diffusion neutron noise solver of APOLLO3® and a theoretical discussion of fission-modes noise," *M&C 2017 - International Conference on Mathematics & Computational Methods Applied to Nuclear Science & Engineering*, Jeju, Korea, April 16-20, 2017, on USB (2017)

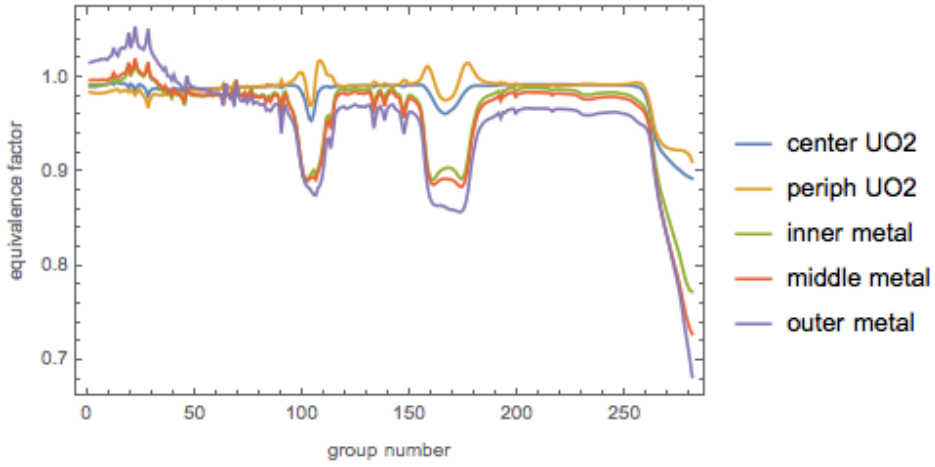

Figure 11: Multigroup equivalence factors of selected fuel pins along the x-axis in a 281-group calculation.

[3] A. Gammicchia et al., "Neutron Kinetics Equations in APOLLO3® Code for Application to Noise Problems," *Submitted to M&C 2019 conference.*

[4] S. Santandrea et al., "A Neutron Transport Characteristics Method for 3D Axially Extruded Geometries Coupled with a Fine Group Self-Shielding Environment," *Nucl. Sci Eng.* **186**, pp 239-276 (2017)

[5] I. Zmijarevic, "Multidimensional Discrete Ordinates Nodal and Characteristics Methods for APOLLO2 Code," *Proc. Int. Conf. on Mathematics and Computation, Reactor Physics and Environmental Analysis in Nuclear Applications (M&C.99)*, Madrid, Spain, Sept. 27-30, 1999.

[6] D. J. Siefman et al., "Full Core modeling techniques for research reactors with irregular geometries using Serpent and PARCS applied to the CROCUS reactor," *Annals of Nuclear Energy*, **85**, 434–443, (2015)

[7] A. Rais et al., "Full neutronic modeling of the CROCUS reactor with SERPENT and PARCS codes," *M&C 2017 - International Conference on Mathematics & Computational Methods Applied to Nuclear Science & Engineering*, Jeju, Korea, April 16-20, 2017, on USB (2017)

[8] E. Brun et al., "TRIPOLI-4®, CEA, EDF and AREVA reference Monte Carlo code," *Ann. Nucl. Energy,* vol. 82, pp. 151-160, 2015.

[9] N. Hfaiedh, A. Santamarina, "Determination of the optimised SHEM mesh for transport calculation," *Proc. Int. Top. Mtg. on Mathematics and Computation, Supercomputing, Reactor Physics and Nuclear and Biological Applications (M&C2005)*, Avignon, France, Sept 12-15, 2005.

[10] R. Sanchez et al., "APOLLO2 Year 2010" *Nucl. Eng and Technology* **42**, pp. 474-499 (2010)

[11] M. Coste-Delclaux, "GALILEE: A Nuclear Data Processing System for Transport, Depletion and Shielding Codes", *Proc. Int. Conf. on Physics of Reactors, "Nuclear Power: A Sustainable Resource," (PHYSOR 2008)*, Interlaken, Switzerland, Sept. 14.19, 2008.

[12] A. Kavenoky. "The SPH HomogenizationMethod.", *Proc. IAEA-OECD A Specialists' Meeting on Homogenization Methods in Reactor Physics*, Lugano, Switzerland, 1978. IAEA-TECDOC-231, Vienna (1980).